Is CF_3I a good gaseous dielectric? A comparative swarm study of CF_3I and SF_6

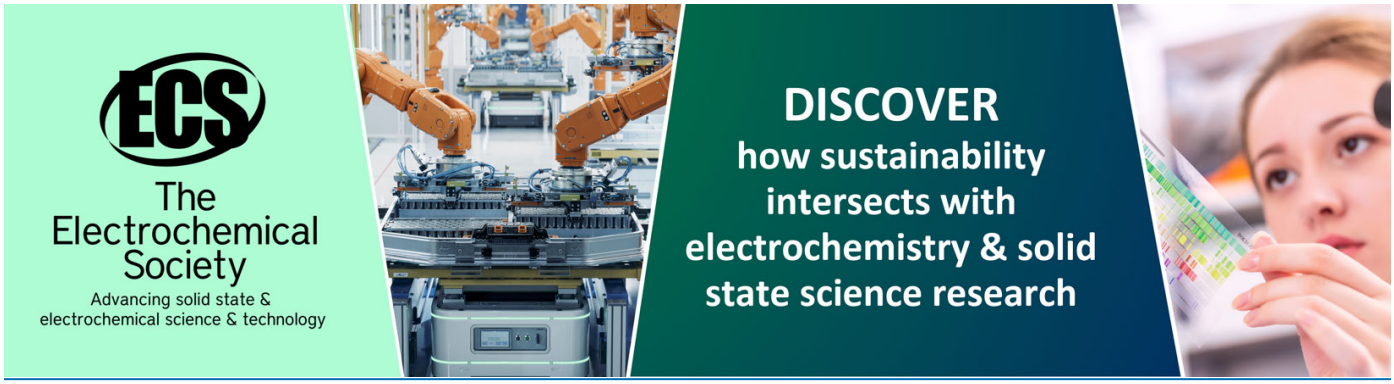

Journal of Physics: Conference Series **86** (2007) 012008 doi:10.1088/1742-6596/86/1/012008

Is CF_3I a good gaseous dielectric? A comparative swarm study of CF_3I and SF_6

J. de Urquijo

Instituto de Ciencias Físicas, Universidad Nacional Autónoma de México, P.O. Box 48-3, 62251 Cuernavaca, Mor., México

jdu@fis.unam.mx

Abstract. This paper deals with the measurement of the electron drift velocity, the longitudinal diffusion coefficient and the effective ionisation coefficient in pure CF_3I and CF_3I mixtures. The E/N range covered was 100-850 Td (1 Td=10^{-17} V cm^2). The present results were derived from a pulsed Townsend experiment. For pure CF_3I, the values of the electron drift velocity and of the effective ionisation coefficient were found to increase steadily with E/N. The E/N value at which ionisation equals attachment, commonly referred to as the limiting field strength, was found to be E/N_{lim}=437 Td, which is higher than that of SF_6 (360 Td), a widely used insulating gas. Moreover, the curve for the mixture of 70% CF_3I with N_2 is very similar to that of SF_6 in the neighbourhood of E/N_{lim}. Thus, from the point of view of these coefficients, CF_3I would seem to be superior in dielectric behaviour to SF_6. Besides, CF_3I is an environmentally friendly gas as opposed to SF_6. Certainly, many more tests should be performed to regard CF_3I as a good dielectric and possible substitute to SF_6.

1. Introduction

Sulphur hexafluoride is probably one of the most extensively used gases because of its many industrial and scientific applications. SF_6 is chemically inert, non-toxic, non-flammable, non-explosive, and thermally stable at temperatures less than 500 C. The outstanding properties of SF_6 make it suitable as an insulating medium in the equipment used for the transmission and distribution of electric power. SF_6 is strongly electronegative, with a high dielectric strength, and a breakdown voltage nearly three times higher than that of air at atmospheric pressure. On the other hand, SF_6 forms highly toxic and corrosive compounds (e.g., S_2F_{10}, SOF_2) when it is subjected to electrical discharges. Sulphur hexafluoride is an efficient infrared (IR) absorber and, due to its chemical inertness, it is not readily removed from the earth's atmosphere. Both these latter properties make SF_6 a potent greenhouse gas, although benign with regard to stratospheric ozone depletion, since it is chemically inert [1]. Since the very first measurements in 1970 [0.03 pptv (1 ppt=1 part in 10^{-12} per volume of atmospheric air)], the purely anthropogenic greenhouse gas SF_6 increased by two orders of magnitude to a global mean value of 2.8 pptv in 1992. While the uncertainties in these numbers make extrapolations difficult, it is clear that the atmospheric concentration of SF_6 is increasing and could reach 10 pptv by the year 2010 and 65 pptv by the year 2100, depending upon the assumptions of release rates [2]. SF_6 has a global warming potential (GWP) of nearly 24,000 times greater than that of CO_2, the predominant contributor to the greenhouse effect, and its atmospheric lifetime in the environment has been estimated around 3,200 years.

The above concerns have moved scientists and engineers into finding possible substitutes for this otherwise formidable gas. Mixtures of SF_6 with fluorocarbon gases, rare gases and atmospheric gases have been tried. Of these, the SF_6-N_2 mixture has been found industrially useful for some high voltage applications. Other fluorocarbons, such as c-C_4F_8 have a higher dielectric strength than that of SF_6, although a GWP of 11,200 and a residence time in the atmosphere of 3,200 years of the former would discard it as a viable substitute gas. .

Trifluoroiodomethane (CF_3I), currently used as an etching gas [3], has been found very recently to be a potential high voltage insulator, both on its own and mixed with N_2 and CO_2 [4,5]. In constrast to SF_6, the global warming potential of CF_3I is less than that of CO_2 (GWP=1), and its lifetime in the atmosphere is very short, estimated to be less than two days, thereby ensuring that CF_3I does not deplete the ozone layer [6]. CF_3I has also found applications as an alternative refrigerant to commonly used fluorocarbons such as CF_4, for example [7]. In spite of the potential importance of CF_3I, there is still a substantial lack of information regarding this molecule. Recent reviews on electron interactions with CF_3I [8,10] indicate that even the cross sections for total electron scattering, attachment and ionization are scarce, and that further research on these matters is called for to either confirm or revise the available data, and also to extend the energy ranges thus far studied. Moreover, one of these recent review [8] states that no data for electron transport, ionization and attachment coefficients are available for this molecule.

This paper presents previously published measurements [11] on the electron drift velocity v_e, the density-normalized longitudinal diffusion coefficient ND_L, and the density-normalized effective ionization coefficient $(\alpha-\eta)/N$ for pure CF_3I and its mixtures (1%-70%) with N_2 (α and η are the electron impact ionization and attachment coefficients, respectively). From the point of view of a possible application of CF_3I as a gaseous dielectric, we compare the above swarm coefficients with those of SF_6, including their limiting field strength.

2. Experimental

The pulsed Townsend apparatus that was used to measure the above parameters has been described in detail elsewhere [12]. A schematic of the apparauts is shown in Fig. 1a. Briefly, the method relies on the time-resolved observation of the total displacement current (electrons, positive and negative ions) moving through a parallel-plate capacitor (12 cm in diameter) filled with the research gas, to which a voltage has been applied to produce a very homogeneous electric field over a central portion of 2 cm diameter. The initial photoelectrons are released by a UV flash from the third harmonic (355 nm) of a Nd-YAG laser. In this experiment the gap distance was kept fixed at 3.1 cm, set to within an accuracy of 0.025 mm.

Prior to filling it with the gas or its mixture, the vacuum vessel was evacuated down to 10^{-6} torr. The range of working pressures was 0.2-20 torr. The gas pressure and mixture composition was measured with an absolute capacitance manometer to an accuracy of 0.01%, while the gas temperature was measured to an accuracy of 0.2% over the range 293-300 K. The CF_3I and N_2 samples both had a quoted purity of 99.9% and 99.999%, respectively, and were introduced into the discharge vessel without further purification. The displacement current was measured with a 40 MHz transimpedance amplifier, and recorded on a 100 MHz digital oscilloscope.

In the presence of electron drift, longitudinal diffusion, ionization and attachment, the temporal development of the electron current within the gap is described by the expression [11]

$$i_e(t) = \frac{n_0 q_o}{2T_e} \exp(\alpha_e v_e t)\left\{\left[1-\phi\left(\frac{(v_e+\alpha_e D_L)t-d}{\sqrt{4D_L t}}\right)\right]+\exp\left(\frac{v_e+\alpha_e D_L}{D_L}d\right)\left[\phi\left(\frac{(v_e+\alpha_e D_L)t+d}{\sqrt{4D_L t}}\right)-1\right]\right\} \quad (1)$$

where n_o is the initial photoelectron number, q_o is the electron charge, d is gap spacing, $T_e=d/v_e$ is the electron transit time, $\alpha_e=\alpha-\eta$, and

$$\phi(x) = \frac{2}{\sqrt{\pi}} \int_0^x exp(-u^2)\, du \,. \tag{2}$$

is the error function of argument *u*. Equation (1) was derived on the assumption of a simultaneous release of the photoelectrons from the cathode at time t=0. Because of the finite laser pulse duration and of the instrumental bandwidth, the rise of the measured electron avalanche is not sharp, yet it displays a Gaussian-like shape resembling that of the laser pulse. On the other hand, the fall is affected by longitudinal diffusion effects which, for fixed E/N, become more apparent as the gas pressure is reduced.

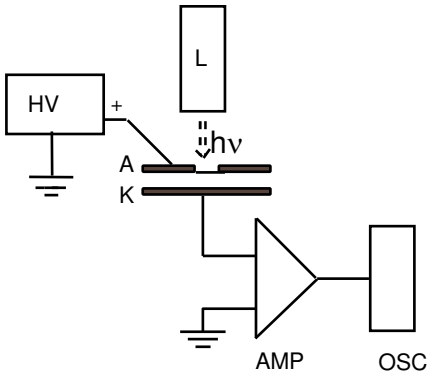

Figure 1. A schematic of the pulsed Townsend apparatus. HV, high voltage Supply; L, laser; A, anode; K, cathode; AMP, transimpedance amplifier; OSC, Digital oscilloscope.

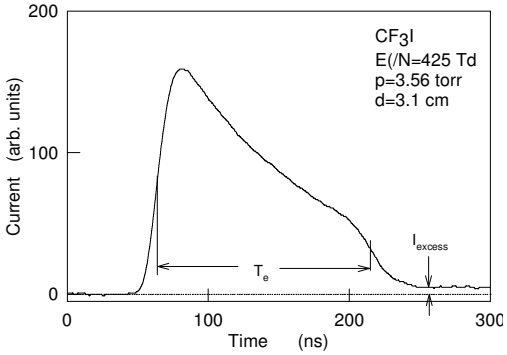

Figure 2. A sample electronic transient of CF_3I. Conditions are indicated at the inset. T_e is the electron transit time and I_{excess} is the current due to the ions (see the text).

When diffusion is either negligible or absent, equation (1) reduces to

$$i_e(t) = \begin{cases} \dfrac{n_0 q_o}{T_e} \exp(\alpha_e v_e t) & 0 \le t \le T_e \\ 0 & t > T_e \end{cases} \tag{3}$$

A result that had been quoted previously [14].

Initial values of v_e and $(\alpha-\eta)/N$ were derived from equation (3) to fit the electron transients. Briefly, the electron transit time T_e is that elapsed between the midpoints of the rising and falling edges of the pulse, from which $v_e=d/T_e$ is calculated, and the density normalized effective ionization coefficient $(\alpha-\eta)/N$ is obtained from a least-squares fitting procedure applied to the rising ($\alpha > \eta$) or falling ($\alpha < \eta$) exponential part of the avalanche. At this point, we would like to note that both v_e and of $(\alpha-\eta)/N$ are obtained simultaneously from the same electron transient. Under some conditions of E/N and N, when α and η are large, the ionic currents during the electron transit may contribute to the

total, measurable current; even though its contribution is relatively small, this can be readily subtracted from the total current by approximating their exponential rise to a straight line, thereby obtaining an even closer measurement of the electron current (see Fig. 2, I_{excess}).

When the above procedure was completed, then full use of equation (1) was made to obtain the longitudinal diffusion coefficient. Usually, corrections to the drift velocity rendered values slightly larger (1-2%), although the effective ionization coefficient remained essentially unchanged. These final values are the ones to be reported below.

3. Measurement of electron swarm coefficients in CF_3I

The swarm coefficients reported in this section correspond to the measurements of electron avalanches over the pressure range 0.4-20 torr, and room temperatures between 293 and 301 K. The uncertainties reported here are the result of averaging a series of measured coefficients for the same E/N value and different pressures. Normally, we used two to five different pressurees. The average uncertainties are 1% for the electron drift velocity, 8% for the longitudinal diffusion coefficients, 9% for the ratio D_L/K_e, where K_e is the electron mobility, and 5% for the effective ionization coefficient, respectively.

3.1 Electron drift velocities

The electron drift velocities, v_e, for CF_3I, CF_3I-N_2 and N_2 are shown plotted in Figure 3 over the range of E/N from 100 to 850 Td. The CF_3I-N_2 mixtures correspond to CF_3I shares of 5%, 10%, 20%, 50% and 70%. The E/N range covered for each CF_3I-N_2 mixture was limited, on the lower part, by the strong attachment of this gas, which precluded the observation of the falling portion of the electron avalanche, while the upper part of the E/N range was limited by the very low pressures used (<0.5 torr), which produced avalanches with substantial contributions from longitudinal diffusion. The drift velocity curves for the 1% and 2% CF_3I-N_2 mixtures have also been measured, but their values over the E/N range used were very similar to those of pure N_2, and thus were omitted for the sake of clarity in the figures presented.

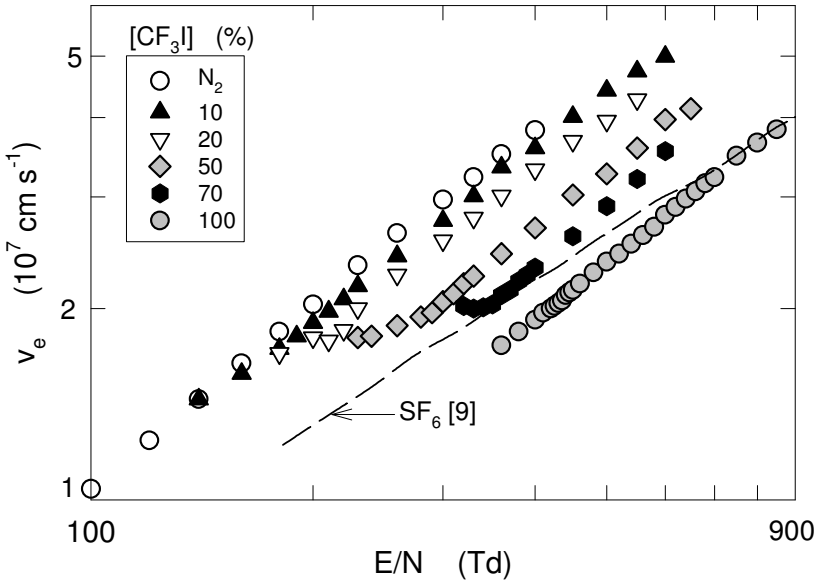

Figure 3. The electron drift velocity in CF_3I and in the CF_3I-N_2mixtures with 5%, 10%, 20%, 50% and 70% CF_3I as a function of E/N [11]. The crosses are the recommended electron drift velocities for SF_6 [9,15]. The SF_6 data are shown only for order-of-magnitude comparison and trend with those of CF_3I and the CF_3I- N_2 mixtures.

For the purpose of comparison with another potent gaseous dielectric, we have also plotted Aswchwanden's values for the drift velocity of electrons in SF_6 [9,15]. It is noted that the values of v_e for SF_6 are higher than those for CF_3I for E/N<700 Td. The calculated momentum transfer cross section for CF_3I [8] is approximately an order of magnitude smaller than the measured cross section of SF_6 over a wide electron energy range [15]. This means that, even considering the larger relative mass of CF_3I (194 Da) with respect to that of SF_6 (146 Da), the electron drift velocity in CF_3I should still be greater than that in SF_6. In view of this, we suggest that the relatively small values of the electron drift velocities in CF_3I with respect to those in SF_6 for E/N<700 Td may be due, additionally, to the stronger polar character of CF_3I as compared to that of SF_6, with dipole polarizabilities of 9.36 $Å^3$ and 6.54 $Å^3$, respectively [16,17].

The electron drift velocities in N_2 were also measured in this study, and found to be in good agreement with previously published data [18]. It is important to note that the 5% and 10% CF_3I-N_2 curves deviate from the N_2 curve, and also that their v_e values become systematically smaller than those of N_2, due to the influence of CF_3I. For CF_3I contents greater than 10%, the v_e curves bear a round curvature over their initial region of E/N, departing from the N_2 curve, and resembling the typical curves of negative differential conductivity [19,20].

To the best of our knowledge, no previous data for the electron drift velocities in either CF_3I or the CF_3I-N_2 mixture have been published before.

3.2 *Longitudinal diffusion coefficients for electrons and the ratio D_L/K_e*

The values of the density-normalized longitudinal diffusion coefficient, ND_L, for electrons in pure CF_3I and in the 5%, 10%, 20%, 50% and 70% CF_3I-N_2 mixtures, have been plotted in Figure 4 as a function of E/N. The ND_L values for the 1% and 2% CF_3I-N_2 mixtures, since these are very close to that of N_2.

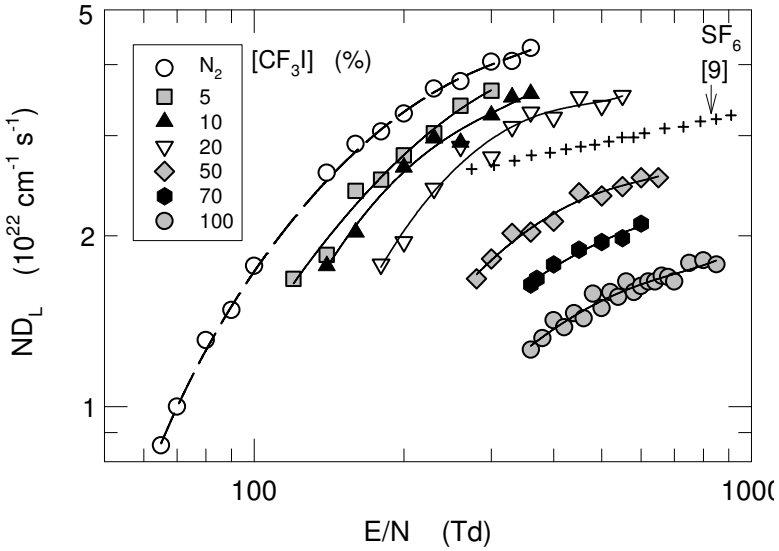

Figure 4. The density-normalized longitudinal diffusion coefficients ND_L for electrons in CF_3I and in the CF_3I-N_2 mixtures with 5%, 10%, 20%, 50% and 70% CF_3I as a function of E/N. For the solid lines through the points, see the curve fittings in Ref. [11]. The crosses are the recommended ND_L values for SF_6 [9,15]. These data are shown only for order-of-magnitude comparison and trend with those of CF_3I and the CF_3I- N_2 mixtures.

A comparison with the ND_L values for SF_6, shows that those for pure CF_3I are smaller than the ones for SF_6 by a factor of about two over the whole E/N range of overlap. Again, for the sake of comparison, the longitudinal diffusion coefficients of Aschwanden [9] for SF_6 are also plotted in this figure.. The different mixtures of CF_3I-N_2 present a similar trend as in the pure case. Moreover, the percentages corresponding to 50% and 70% of CF_3I have values smaller that those for SF_6. To the best our knowledge, no previous values of ND_L have been published.

A coefficient that provides a measure of the translational energy of the charge carriers as a function of E/N is the ratio between the density-normalized longitudinal diffusion coefficient and the electron mobility, D_L/K_e, with $K_e=v_e/E$. This ratio is shown plotted in Figure 5, together with the corresponding values for the mixtures as a function of E/N. The D_L/K_e values for SF_6 shown in this figure for the purpose of comparison are, as in the case for ND_L, higher than those for CF_3I by a factor between 1.5 and 2.

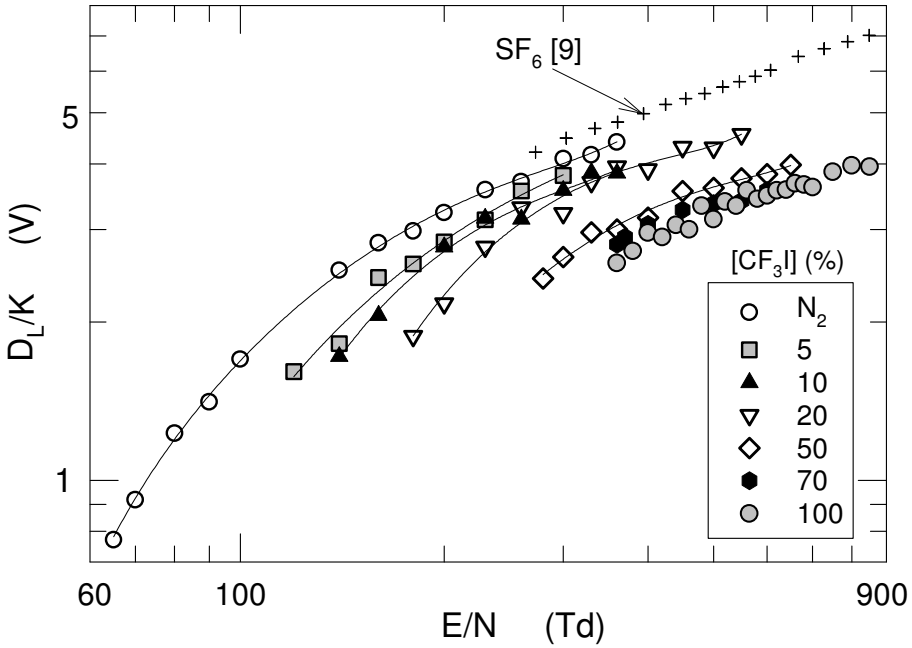

Figure 5. The ratio between the longitudinal diffusion coefficient and the electron mobility, D_L/K_e, for electrons in CF_3I and in the CF_3I-N_2 mixtures. The solid lines through the points represent a curve fitting described in Ref. [11]. The crosses are the D_L/K_e values for SF_6 [9,15], shown here for the purpose of comparing the relative magnitudes of this parameter in SF_6 with those of CF_3I and the CF_3I- N_2 mixtures.

3.3 Effective ionization coefficients and rates

The effective ionization coefficients $(\alpha-\eta)/N$ in CF_3I and in the mixtures of this gas with N_2 are plotted in Figure 6 for the mixtures with low concentration of CF_3I in N_2, and in figure 7 for the 10%, 20%, 50%, 70% CF_3I-N_2 mixtures, all as a function of E/N. Again, the lower limit of our measurements of $(\alpha-\eta)/N$ was due to the impossibility of assessing the electron transit time and hence determine both v_e and $(\alpha-\eta)$, since the strong attachment produced a fast decaying signal that precluded us from measuring the electron transit time. The values of $(\alpha-\eta)/N$ in N_2 and 1%, 2% and 5% CF_3I-N_2 have been plotted separately, in figure 6, to emphasize the increase in $(\alpha-\eta)/N$ for E/N>230 Td with respect to the values of α/N for pure N_2. This effect is mainly due to the fact that the ionization potential of CF_3I is lower (10.23 eV) than that of N_2 (15.58 eV). On the other hand, Figure 7 shows the values of $(\alpha-\eta)/N$ for pure CF_3I and for the 10%, 20%, 50%, 70% CF_3I-N_2 mixtures.

Interestingly, the trend of the $(\alpha-\eta)/N$ values for CF_3I runs almost parallel to that of SF_6. An interesting feature of this curve is the value of the limiting (or critical) field strength, E/N_{lim}, which is defined as that value of E/N at which ionization equals attachment, that is, $(\alpha-\eta)/N=0$. A value of E/N_{lim}=437 Td is measured for CF_3I, which turns out to be significantly higher than that of E/N_{lim}=361 Td for SF_6, an important and widely used high voltage gas insulator [15]. From this point of view, it would then be likely that CF_3I be considered as a viable substitute for SF_6, since it bears the good insulating properties of the latter, besides its non-ozone depleting effects and significantly low global warming potential, in contrast to those of SF_6. Moreover, note that the 70% CF_3I-N_2 curve is essentially the same as that for SF_6 over the whole E/N range of overlap, up to E/N=550 Td.

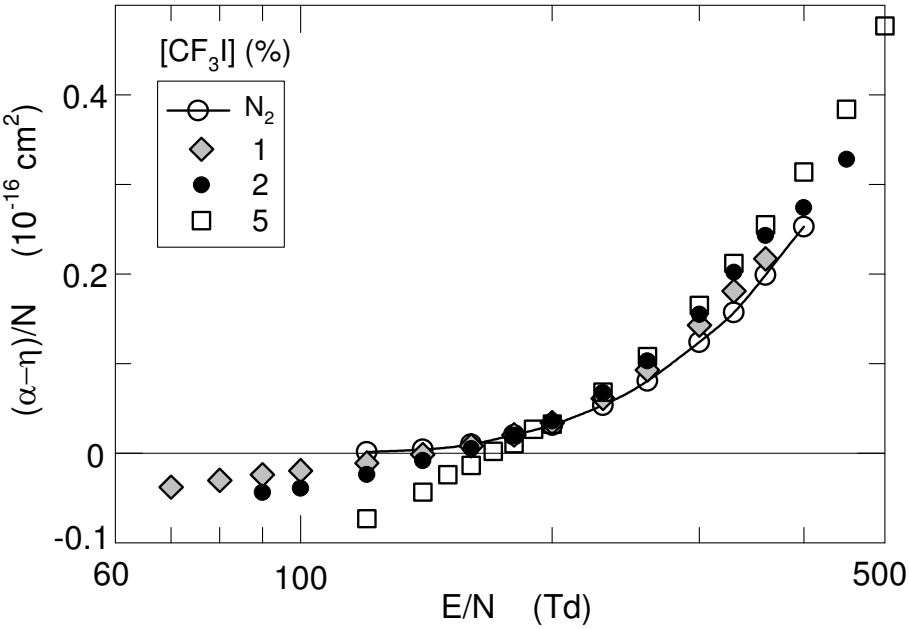

Figure 6. The density-normalized effective ionization coefficients $(\alpha-\eta)/N$ for N_2 and for the CF_3I-N_2 mixtures with 1%, 2% and 5% CF_3I as a function of E/N.

Our experiment could only render effective ionization coefficients. At this stage, we have not been able to assess any particular ionization or attachment coefficients. However, we would like to mention that the only measurements of Jiao et al on the electron impact ionization of CF_3I [21] indicate that the ions formed are CF_3I^+, CF_2I^+, CF_3^+, CF_2^+, CF^+, and I^+, with CF_3I^+ as the predominant positive ion species for electron energies up to 70 eV, followed by I^+, CF_3^+, CF_2I^+, CF_2^+, CF^+, the cross sections of these latter two being a factor of ten smaller than the former three.

As regards negative ions from CF_3I, the strongly electronegative character of this gas stems from the fact that electron attachment to CF_3I proceeds dissociatively via the formation of I^-, F^- and CF_3^- and FI^- via two dissociating negative ion states at ~0 eV and 3.8 eV [8]. According to our D_L/K_e data, which provide a rough measure of the average energy of the electron swarm, it is likely that in our experiment both I^- and F^- are formed. It is known that I^- is formed by the zero-eV process via the reaction [8]

$$e + CF_3I \rightarrow I^- + CF_3 \qquad (4)$$

while F^- and CF_3^- are formed by the 3.8 eV process via the reactions

$$e + CF_3I \rightarrow F^- + CF_2I \quad (5)$$

$$e + CF_3I \rightarrow CF_3^- + I \quad (6)$$

Very recently, using several variants of the laser photoelectron attachment method, Marienfeld et al [22] have measured and calculated the dissociative electron impact attachment cross sections to CF_3I molecules leading to I^- formation over the energy range 0.5–500 meV.

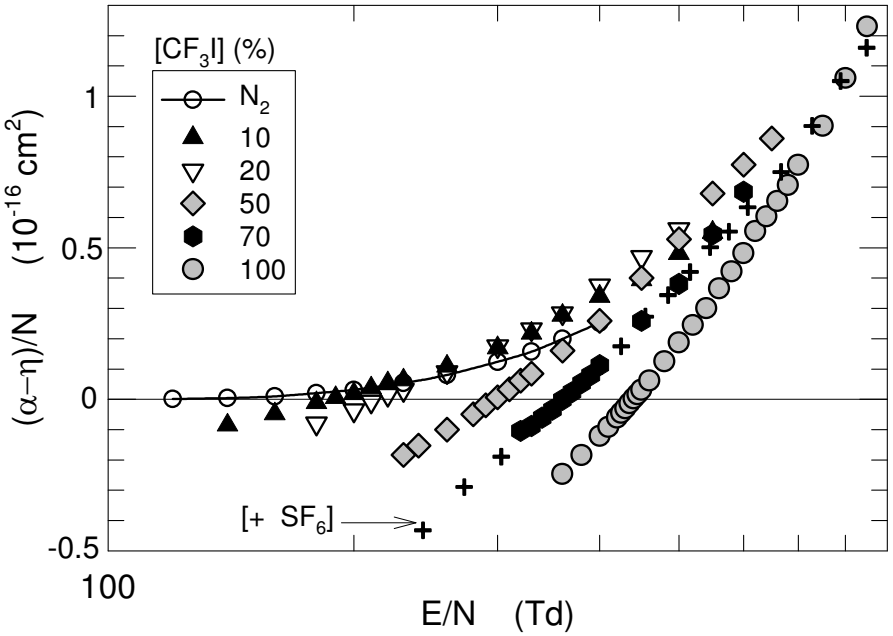

Figure 7. The density-normalized effective ionization coefficients (α–η)/N for CF_3I and in the CF_3I-N_2 mixtures with 5%, 10%, 20%, 50% and 70% CF_3I as a function of E/N. The solid line through the N_2 curve represents a fitting according to Ref. [11]. The crosses are the recommended (α–η)/N values for SF_6 [9,15]. These latter data are shown only for the purpose of comparing the more electronegative character of CF_3I and its mixtures with N_2 with respect to that of SF_6.

Moreover, the mixture with 70% of CF_3I in N_2 runs almost over the corresponding values of SF_6. The practical value of this situation is that an environmentally friendly mixture of CF_3I in N_2 may have the same efficiency as an insulating gas mixture as compared to that of the much less environmentally friendly case of SF_6. To the best of our knowledge, no measurements of the effective ionization coefficient have been published previously.

3.4 Limiting values of E/N

Figure 6 presents the so called *limiting* or *critical* field strength values of E/N_{lim} at which $\alpha=\eta$ for all the CF_3I-N_2 mixtures studied, including that of pure CF_3I. A comparison with the well known E/N_{lim} values for the SF_6-N_2 mixture reveals that for CF_3I concentrations in CF_3I-N_2 the mixture lower than 60%, the SF_6-N_2 mixture is superior, although this limit the CF_3I-N_2 mixture is superior to that of SF_6-N_2. In fact, as judged from these swarm properties, the 70%CF_3I-N_2 mixture is even superior to that of pure SF_6.

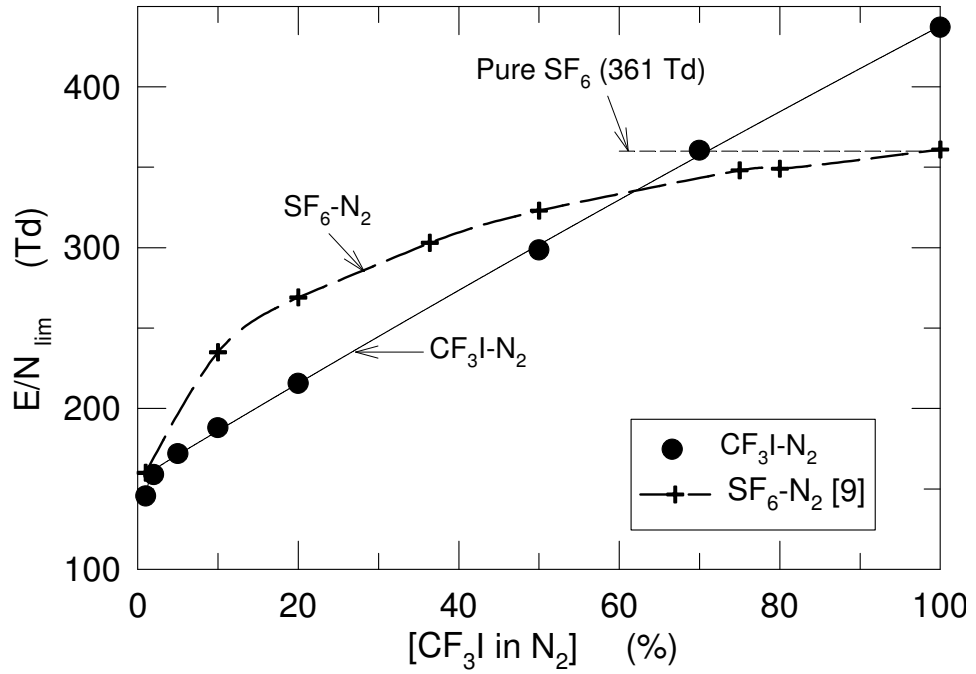

Figure 8. The limiting or critical field strength, E/N_{lim} for the CF_3I-N_2 mixtures. For the purposes of comparison, the values of E/N_{lim} for the SF_6-N_2 mixture have been included.

4. Conclusion

We have used previously published data [11] of the electron transport and ionisation coefficients in CF_3I and CF_3I-N_2 mixtures, covering a wide range of E/N. In this paper we have presented a compariosn of such coefficients with those of SF_6, in the aim to evalute them from the point of view of assessing CF_3I as a possible substitute of SF_6. In particular, we have found that the limiting field strength of pure CF_3I (E/N_{lim} = 437 Td) is higher than that of SF_6 (E/Nlim = 361 Td). An encouraging aspect of the measurements for the mixtures of CF_3I in N_2 presented here is that CF_3I or its mixture with N_2 both have the good properties to be regarded as viable gaseous dielectrics, in consonance with recent research in this direction indicating that CF_3I or its mixture with N_2 would be viable gaseous dielectrics since the mixture with 70% CF_3I presents a very similar behaviour to that of pure SF_6. Admittedly, many other chemical, thermal and economical studies are needed to consider CF_3I or its mixtures with N_2 as real substitutes for SF_6 in high voltage and switchgear applications.

In view of the scarcity of data on the interaction of these gases with electrons, we hope the present data will be useful for testing the available relevant cross sections, or even to attempt deriving the first sets.

Acknowledgements

This work was supported by Project PAPIIT IN102305. Thanks are due to A. Bustos and R. Bustos for their technical assistance.

References

[1] Christophorou L G and Olthoff J K and Green D S 1997 *NIST Technical Note 1425* Washington: U.S. Government Printing Office

[2] Hope C 2003 *The marginal impacts of CO2, CH4 and SF6 emissions;* www.ofgem.gov.uk/sustainability/Environmnt/Policy/Documents/3281-hope_report.pdf;

Judge Institute of Management, University of Cambridge
[3] Misra A, Sees J, Hall L, Levy RA, Zaitsev VB, Aryusook K, Ravindranath C, Sigal V, Kesari S, Rufin D 1998 **,** *Materials Letters* **34,** 415
[4] Nakauchi S, Tosu D, Matsuoka S, Kumada A, Hidaka K 2006 Proc. XVI Int. Conf. Gas Disch. and Appl. Vol 1 pp 365-369 Xi'an, China
[5] Taki M, Hiromi O, Maekawa D, Mizoguchi H, Yanabu S 2006 Proc. XVI Int. Conf. Gas Disch. and Appl. Vol 2 pp 793-796 Xi'an, China
[6] Solomon S, Burkholder J B, Ravishankra A R, and. García R R 1994 *J. Geophys. Res. D* **99** 20929
[7] Duan Y Y, Shi L, Sun L Q, Zhu M S and Han L Z 2000 *Int. J. Thermophys.* **21** 393
[8] Christophorou L G and Olthoff JK 2000 *J. Phys. Chem. Ref. Data*, **29** 553
[9] Aschwanden Th 1985, *in Gaseous Dielectrics IV*, ed L G Christophorou *et al* (New York: Pergamon) p 24
[10] Rozum I, Limão-Vieira P, Eden S, Tennyson J, and Mason N J 2006 *J. Phys. Chem. Ref. Data* **35**, 267
[11] de Urquijo J, Juárez A M, Basurto E and Hernández-Ávila J L 2007 *J. Phys. D* **40** 2205
[12] Hernández-Ávila J L, Basurto E, and de Urquijo J 2002 *J. Phys. D* **35** 2264
[13] Brambring J 1964 *Z Physik* **179** 532
[14] Raether H 1964 *Electron Avalanches and Breakdown in Gases* (London: Butterworths)
[15] Christophorou LG, and Olthoff JK 2000 *J. Phys. Chem. Ref. Data* **29,** 267
[16] Glen RC 1994 *J. Comp.-Aided Mol. Design*, **8** 457
[17] Lide, DR 2001 (Ed.) *Handbook of Chemistry and Physics*, 73rd ed., CRC Press
[18] Dutton J 1975 *J. Phys. Chem. Ref. Data* **4**, 577
[19] Petrović, Z Lj, Crompton R W; Haddad G N 1984 Australian Journal of Physics, **37**, 23
[20] Vrhovac, Slobodan B, Petrović Z Lj 1996 Physical Review E , **53**, 4012-4025
[21] Jiao CQ, Garscadden A, Ganguly B, Dejoseph CA 2000 *American Physical Society, 53rd Annual Gaseous Electronics Conference* October 24-27 Houston, Texas Meeting abstract KR1.006
[22] Marienfeld S, Fabrikant I I, Braun M, Ruf M-W and Hotop H, *J. Phys. B* **39**, 105 (2006)